13th International Symposium on Turbulence and Shear Flow Phenomena (TSFP13)
Montreal, Canada, June 25–28, 2024

COUPLING OF WALL-PRESSURE FLUCTUATIONS IN A TRANSPIRATIVELY-COOLED TURBULENT BOUNDARY LAYER

Sophie Hillcoat
Department of Mechanical and Mechatronics Engineering
University of Waterloo
Waterloo, Ontario, Canada
srhillcoat@uwaterloo.ca

Jean-Pierre Hickey
Department of Mechanical and Mechatronics Engineering
University of Waterloo
Waterloo, Ontario, Canada
j6hickey@uwaterloo.ca

ABSTRACT

Transpiration cooling is a thermal protection system under active development for external aerothermal heating applications. Pressure-driven coolant flow is effused through a porous wall into a hot turbulent boundary layer. This work investigates the influence of the wall-pressure fluctuations on the coupling between the hot boundary layer and the porous media flow. Using a pore network model, two potential learning-based transfer functions (linear regression and neural network) to approximate the flow in the porous medium are developed and coupled to a high-fidelity direct numerical simulation (DNS) of a compressible turbulent boundary layer.

It was found that the coupling implemented using a linear regression-derived expression was unable to properly characterize the flow in the porous domain in instances of large variation in pressure, highlighting the importance of incorporating the spatial influence of neighbouring pores. Consequently, the implementation of this expression in the direct numerical simulation resulted in a decorrelation of the pressure signal at the wall and consequently an artificial smoothing of the fluctuations. The direct numerical simulation coupled with the neural network, which did incorporate the influence of neighbouring pores, was more successful. The highest frequency pressure fluctuations were attenuated in roughly the first quarter of the transpiration region due to the spatial interactions within the porous medium flow, whereas the lower frequency fluctuations persisted throughout the entirety of the domain. The neural network case also demonstrated reduced sensitivity to the coupling between pressure and injection velocity as compared to the linear regression case, which was reflected both in the blowing ratio distribution in the transpiration region as well as in the obtained wall-normal velocity and pressure fluctuation cross-correlations.

INTRODUCTION

Thermal protection systems (TPS) are a key technology to enable the use of lower cost and lighter materials for high-speed vehicle applications. Active TPS such as transpiration cooling is used to minimize thermal loading and is being actively investigated for high-speed external aerodynamic applications (Esser *et al.*, 2016). By effusing a coolant through a porous side wall, transpiration cooling combines the convective cooling within the porous wall with the formation of a thermal buffer in the boundary layer insulating the wall from the high-enthalpy external flow. Consequently, this technique has the potential to be more effective than other mass-injection active TPS such as film or convective cooling (Eckert & Livingood, 1954).

The effectiveness of transpiration cooling systems is directly tied to the mass flow rate of coolant injected through the porous wall (Christopher *et al.*, 2020). Furthermore, as the coolant is injected into a boundary layer, there is a direct hydrodynamic coupling between the effused coolant and the external flow. This hydrodynamic coupling can be leveraged to reduce drag in a laminar boundary layer (Jiao & Floryan, 2021) or modify the location of transition to turbulence (Cerminara, 2023). The injected mass flow rate also impacts the formation of coherent structures in the downstream flow (Zhang *et al.*, 2022). Although Gülhan & Braun (2011) showed greater effectiveness of transpiration cooling in a laminar versus turbulent boundary in hypersonic flows, many modern applications to fully turbulent flows are used for TPS (Zhu *et al.*, 2018). Some applications of turbulent TPS leverage the thermal degradation of hydrocarbon fuels (Liu *et al.*, 2023) and can be integrated as a face plate injector (Jin *et al.*, 2023).

Predictive simulations of transpiration cooling are critical for optimal design considerations. On the one hand, we seek to reduce the pressure drop required to drive the flow and minimize the coolant's momentum into the boundary layer, thus minimizing turbulent mixing. Turbulent mixing should be minimized between the coolant and hot gas streams as it can impede the extent of the thermal buffer layer. As the momentum of the coolant into the boundary layer is reduced, the relative importance of the turbulent fluctuations at the outlet of the porous wall cannot be neglected. These wall pressure fluctuations are naturally occurring in a turbulent boundary layer and can be characterized by well-established pressure spectra (see, e.g. Grasso *et al.* (2021, 2019); Hillcoat & Hickey (2021)). This is particularly important as regions of

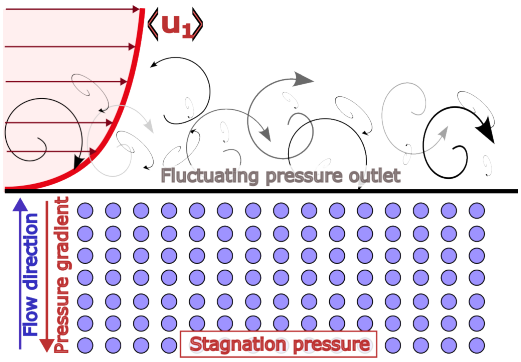

Figure 1. Schematic illustration of the coupling between the two domains in transpiration cooling (the turbulent boundary layer and the porous wall).

higher wall pressure impede the flow, which gets diverted in the porous medium to other zones of lower pressure. Given the effectively incompressible flow within the porous medium, the information transfer is nearly instantaneous.

This strong coupling is schematically represented in figure 1. The coolant is driven through the porous medium due to an imposed pressure gradient, which in turn varies locally due to spatio-temporal pressure fluctuations arising from the turbulence. Consequentially the local mass flow rate of coolant is influenced by the pressure fluctuations in the turbulent boundary layer, and vice-versa.

Transpiration cooling systems present a significant challenge to simulate due to the large range of length and time scales that must be resolved to fully capture both the external flow and the flow in the porous medium. Doing so quickly becomes prohibitively computationally expensive. Generally speaking, there are three treatments of the porous medium and coolant injection that are used in the literature:

1. A monolithic approach that fully resolves both the porous medium and the turbulent flow domain. Examples of this approach are very few and are necessarily limited in the size, number, and geometry of pores considered, such as the work done by Cerminara *et al.* (2020) and Zhang *et al.* (2022). Although not an example of transpiration cooling due to the lack of coolant injection (blowing), the relevant work done in modeling turbulent boundary layer flow over a porous medium (such as that done by Wang *et al.* (2022)) should also be recognized as it nonetheless provides valuable information on the interaction between these two fluid domains.
2. A bulk medium approach wherein the flow through individual pores of the porous medium is not resolved and the bulk flow through the medium is instead modeled using the Darcy-Forchheimer relationship. There are multiple examples of this approach, which consists two alternating solvers; one which solves for the flow in hot gas domain, and a finite-difference solver which handles the porous domain (ex. König *et al.* (2021); Dahmen *et al.* (2014); Prokein (2021)). Notably, all examples of this method found by the authors employed a RANS model to simulate the main flow domain and consequently are not able to resolve the turbulent structures formed in the boundary layer and the corresponding coupling between pressure and velocity fluctuations at the interface.
3. A decoupled boundary condition approach wherein the porous medium is not modeled and transpiration is simulated by way of a constant or mass flux boundary condition (uniform or spatially-varying) at the porous wall. While this method has the disadvantage of not considering the coupling and interactions between the two flow domains, it does allow for insight into the impact of coolant injection on the turbulent boundary layer, such as seen in Christopher *et al.* (2020) and Cerminara (2023).

The present work proposes a compromise between these three approaches that allows for a highly-resolved direct numerical simulation of the turbulent boundary that incorporates the coupling with the porous medium while easing the aforementioned limits on the size and quantity of pores considered. Using this method, the fundamental pressure coupling between the transpirative wall and the hydrodynamic pressure of the turbulent boundary layer is investigated in order to uncover the underlying dynamics of a variable pressure field on the flow through the porous medium.

METHODOLOGY

In order to achieve the above goal, the direct numerical simulation code Hybrid is used to obtain a high-fidelity simulation of a turbulent boundary flow over a flat plate (Bermejo-Moreno *et al.*, 2013). This code was previously extended by Christopher *et al.* (2020) to account for transpiration cooling by imposing a constant wall-normal velocity boundary condition over part of the flat plate to mimic the injection of coolant.

In the present work, this constant velocity boundary condition is replaced by a function relating the local coolant injection velocity to the pressure at the wall. This function encapsulates the flow through the porous medium without the computational overhead of a separate solver. The mean rate of coolant injection is set indirectly by specifying a constant coolant reservoir pressure used to calculate the pressure drop across the porous medium.

In order to obtain this function, a pore-network model of a simple cubic lattice porous network is used to simulate the local coolant velocity at the surface pores of the medium with a random pressure signal applied to the surface. A function that can be integrated into the direct numerical simulation code is then derived from this data using two different methods: a linear regression, and a convolutional neural network.

NUMERICAL DETAILS
DIRECT NUMERICAL SIMULATION

The direct numerical simulation (DNS) is conducted using Hybrid, a high-order finite difference solver that computes the compressible Navier-Stokes equations with variable viscosity (Bermejo-Moreno *et al.*, 2013); the equation set is closed with the ideal gas law. The high-order numerical methods and filtering can be stabilized in regions with large gradients using a high-order WENO scheme.

Using the extensions to the code base previously done by Christopher *et al.* (2020), modifications were made to indirectly couple the local injection momentum at the porous wall to a pore-network model of a simple porous medium. The computational domain and turbulent boundary layer inlet boundary conditions are identical to those described by Christopher *et al.* (2020), allowing for a comparison of the results with the pressure/velocity coupling with the constant injection case without having to re-run the uniform injection DNS case.

The average velocities and Reynolds stresses are taken from an established DNS of an incompressible boundary layer

with $Re_\tau = 450$ (Jiménez *et al.*, 2010). The domain is $60\delta_i$ long in the streamwise direction with a height and width of $6\delta_i$, where δ_i is the inlet boundary layer thickness and is set to unity. A fully-structured mesh with wall-normal grid refinement and a size of $2560 \times 180 \times 256$ points was used for all cases. The lower wall is highly cooled, with a set constant temperature of $T_w = 0.5$ compared to the free-stream temperature $T_\infty = 1$. The dependance of the viscosity of the fluid on temperature is accounted for by the power law $\mu = \mu_{ref}(T/T_{ref})^{0.75}$.

The top wall of the domain is assigned an inlet/outlet boundary condition, and the domain is periodic along the transverse (z) axis. At the lower wall a no-slip condition is applied in the x and z direction while the injection of coolant is set by specifying the wall-normal velocity at the boundary. The coolant is assumed to be injected in a laminar state over the region $30 < x < 50$.

PORE-NETWORK MODEL

Darcy flow is assumed in the porous medium due to the small pore sizes and low flow velocities employed in transpiration cooling. Given the simplified flow conditions and to afford a greater computational tractability the pore-network modeling framework OpenPNM (Gostick *et al.*, 2016) was used. Pore network modeling abstracts the porous media as a system of equivalent pipe flows whose pressure drop can be analytically defined by the Hagen-Poiseuille equation. This simplification enables significant computational savings that can be used to increase the heterogeneity or size of the model.

Herein, we defined a cubic lattice of 2.2 million pores ($200 \times 43 \times 256$), with a homogeneous spacing corresponding to the DNS grid spacing and a normal distribution of pore diameters with mean size of 0.0115 and standard deviation of 0.0010. The applied pressure at the porous medium inlet is set to 8.88733 such that the average flow velocity exiting the wall is 0.003 as calculated using the mean wall pressure in the transpiration region from the constant injection DNS case as the wall surface pressure. This value was chosen as it corresponds to the constant velocity boundary condition set in the uniform blowing DNS case to which the DNS results with coupling will be compared. The porous medium was assumed to be at a uniform temperature corresponding to the wall temperature in the DNS cases.

In order to ensure compatibility with the DNS, the same non-dimensionalization is used in OpenPNM as is implemented in Hybrid; the velocity is normalized by the free-stream velocity and distance is normalized by imposing a unitary boundary layer thickness at the inlet. The thermodynamics are non-dimensionalized with the free-stream density and temperature with a consistency non-dimensionalization for pressure.

The coolant velocity at each pore on the surface of the medium was simulated a total of 549 times in OpenPNM, each time with a different pressure signal boundary condition applied to the surface. The pressure signal itself is obtained by assigning a random pressure value to each surface pore. The random values are pulled from a normal distribution with the same mean and standard deviation as the pressure signal in the constant injection DNS case.

LINEAR REGRESSION

A linear regression was performed to obtain an expression relating the surface pressure to the corresponding flow velocity at each pore. Following from Darcy's law, it is expected that the flow velocity exiting a surface pore will have a linear relationship with the local pressure gradient across the porous wall. Such a relationship was observed in porous flow simulations with uniformly sized pores; however, in simulations with a normal distribution of pore sizes this relationship is obfuscated by the corresponding variation in pore hydraulic conductance values through the network. A linear best fit of the surface pressure and velocity fluctuations for each surface pore was performed, and it was found that the slope and offset of the fit showed a strong linear relationship with the hydraulic conductance of the surface pore.

It is therefore only necessary to consider the effect of hydraulic conductance of the surface pore and that of internal pores in the network can be neglected, allowing a multivariable linear regression to be used to obtain an expression of the form $v = C_1\Delta p + C_2 g\Delta p + C_3 g + C_4$, where g is the Hagen-Poiseuille hydraulic conductance of the surface pore, v is flow exit velocity at the pore, and Δp is the wall pressure at the pore. C_1, C_2, C_3, C_4 are constants obtained from the linear regression and are anticipated to be unique to the porous structure being considered.

Despite a very strong R^2 value (0.97) the expression obtained using a linear regression displayed poor performance, with a root mean square (RMS) error 7.59e−4 (roughly 25% of the mean injection velocity). The maximum error was in excess of 265% of the mean injection velocity. The reason for this large error is that the expression obtained via linear regression does not consider the influence of neighbouring pores. Due to the connectivity of the pores within the porous medium, an increase in local pressure that impedes the flow at one pore will result in additional flow at the neighbouring pores where the pressure is lower due to the redirection of the flow. This spatial zone of influence is thus critical to analysing the flow distribution.

NEURAL NETWORK

In order to try to capture the spatial components of the relationship between pressure gradient and pore exit velocity that was neglected in the linear regression, a shallow convolutional neural network was developed. Convolutional neural networks (CNN) perform convolution operations on the input data in order to incorporate spatial information and have seen a lot of recent use in image processing and computer vision applications.

The designed network was kept as small as possible in order to mitigate the overhead increase when incorporated into the DNS code. In its final form it has three convolution layers of decreasing kernel size followed by two fully-connected linear layers. Between each operation a rectified linear activation layer is added. As inputs the network takes two 7x7 "images" containing the pressure and hydraulic conductivity data, respectively, for the pore of interest and its 3 adjacent neighbours on all sides. The network then outputs a velocity value for the central pore.

Built using PyTorch, the network was trained for 30 epochs using the Adam optimizer and a root mean square (RMS) loss function. Following the final epoch, the network was applied to the testing dataset, where it had a RMS error of 3.57e−4 (roughly 12% of the mean injection velocity), showing significant improvement compared to the linear regression. This performance improvement is further confirmed by a comparison of the error histograms of the neural network and linear regression when applied to the same testing dataset (figure 3).

It is possible that the neural network's performance could be further improved by increasing the extent of neighbours considered for each pore, however this comes at a significant

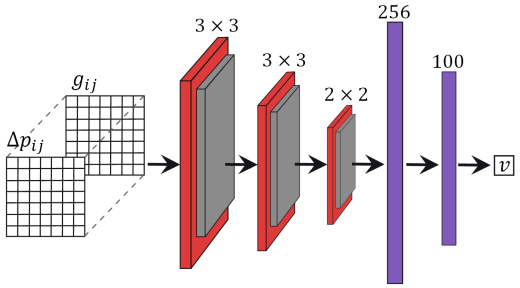

Figure 2. Neural network structure. The red blocks correspond to convolution layers with the indicated kernel size. The grey blocks are rectified linear activation (ReLU) layers, and the purple blocks are fully connected linear layers of the indicated size.

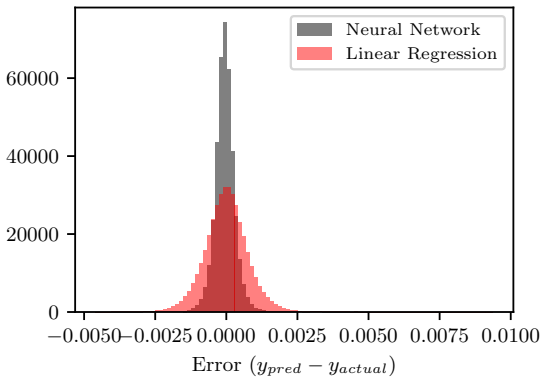

Figure 3. Histogram of the error of the linear regression and neural network respectively when applied to the testing data set.

computational penalty. As the purpose of using the neural network was to minimize the additional computational cost compared to directly coupling a porous medium solver, it was decided that the present performance was sufficient.

RESULTS

The results from four distinct cases are considered and compared herein:

1. A no blowing case, wherein there is not injection at the porous wall and the problem reduces to a turbulent boundary layer over a constant temperature flatplate.
2. A uniform blowing case, wherein the injection velocity at the porous wall is set a priori and is constant for all pores. This case corresponds to the Uniform-0.6% case done by Christopher *et al.* (2020) with a set blowing ratio $F = \bar{\rho}_c v_c / \bar{\rho}_\infty U_\infty$ of 0.6%.
3. A blowing case using the linear regression expression to indirectly couple the main domain and the flow in the porous medium.
4. A blowing case using the shallow convolutional neural network to indirectly couple the main domain and the flow in the porous medium.

The numerical performance of the linear regression case was comparable to that of the first two cases, however, the neural network case did impose a significant performance penalty, requiring roughly 3 times the walltime as the other cases for

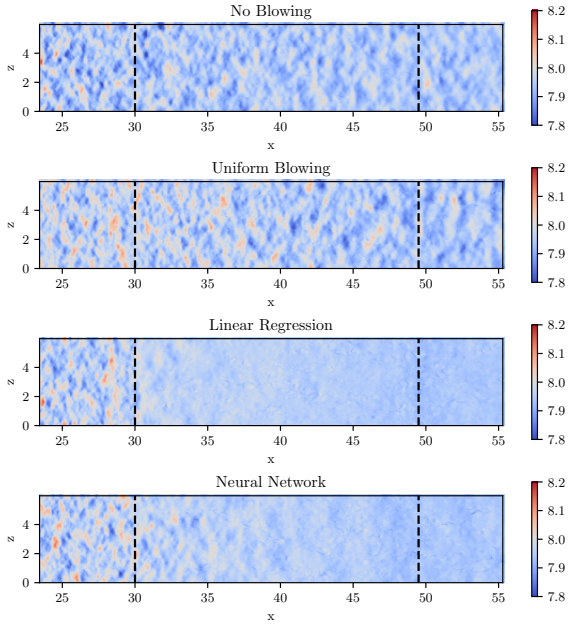

Figure 4. Pressure signal snapshots at the wall. The dashed black lines indicate the beginning and end of the transpiration region.

the same number of time steps. It is however expected that this penalty can be reduced through more strategic division of the computational domain for parallelization, which will be implemented going forwards. Each of the cases considered were run for over 3 flow-through times to ensure convergence.

Snapshots of the pressure signal just above the wall in the vicinity of the transpiration region for all cases are shown in figure 4. It is immediately apparent that the coupling of the wall pressure and injection velocity results in an attenuation of the pressure fluctuations within and even downstream of the transpiration region. This effect appears to be more pronounced in the linear regression case, however it is theorized that this is an artifact of the reduced accuracy of the linear regression coupling. Due to not taking into account the influence of neighbouring pores, the expression obtained via linear expressions yields large errors in regions where the surrounding pressure deviates significantly from the mean. Due to these errors, the larger scale pressure correlations are not adequately captured and thus appear to be attenuated in the results.

In contrast, the neural network case is better able to capture the larger pressure correlations as its inclusion of spatial effects significantly reduces the error in its calculated values. The higher frequency pressure fluctuations are attenuated in roughly the first quarter of the transpiration region due to the interaction of the coolant flow at each pore with that of its nearby neighbours. The larger pressure footprints, however, persist throughout the transpiration region.

These observations are corroborated by the mean pressure signal at the wall in the transpiration region (figure 5). As expected, all cases with coolant injection demonstrate an increased pressure at the beginning of the injection region due to the initial interaction of the coolant with the oncoming main flow. In the linear regression case the major pressure fluctuations are quickly lost due the decorrelation of the pressure signal as previously described, however, the largest of these persist in the neural network case, albeit at a reduced amplitude compared to the case of uniform injection. Further investigation is required to determine if this reduction in amplitude

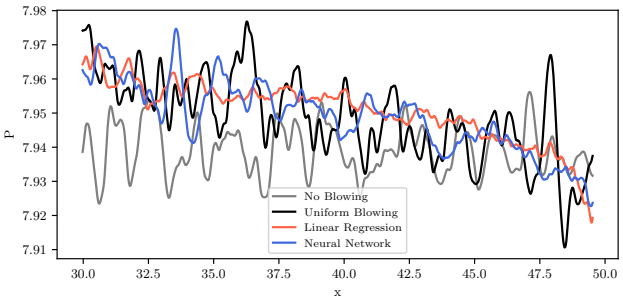

Figure 5. Span-averaged pressure at the wall in the transpiration region.

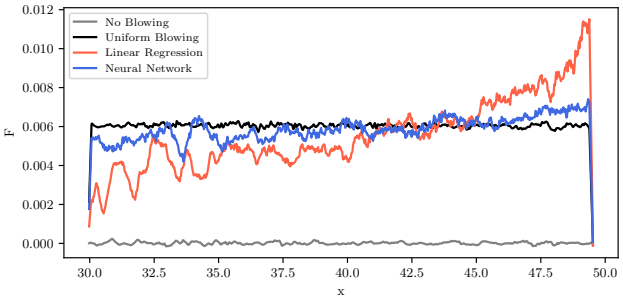

Figure 6. Span-averaged blowing ratio in the transpiration region.

is a physical result due to the coupling, or if they are being obfuscated due to the errors that persist even when using the neural network.

Figure 6 shows the impact of the pressure-velocity coupling on the resultant time and span-averaged blowing ratio. The linear regression case has significantly reduced blowing at the beginning of the transpiration region due to the aforementioned higher pressure zone there. The blowing ratio then increases downstream until it actually exceeds that of the uniform blowing case near the end of the transpiration region, experiencing a sharp spike in the injected coolant at the trailing end. While the neural network case displays the same general trend of beginning with a reduced blowing ratio that increases downstream, the change is much slower and the observed spike just before $x = 50$ is absent. It is clear that incorporating the influence of neighbouring pores significantly decreases the sensitivity of the coupling between pressure and coolant injection.

Figures 7 and 8 plot the negative normalized cross-correlation between the coolant injection velocity and the surface pressure fluctuations for all considered cases at varying distances from the wall and portions of the transpiration region, respectively. In both cases, the horizontal axis r represents the streamwise lag. The pressure fluctuations and wall-normal velocity have a strong negative correlation at the wall which is expected, as this opposing relationship is imposed by the boundary condition used to set blowing (high pressure results in reduced coolant injection). The linear regression case demonstrates a higher degree of correlation than the neural network case due to the lack of influence of neighbouring pores. Interestingly, the strength of this correlation is reduced in the latter half of the transpiration region (dashed line) as compared to the former, although the reason for this is not clear.

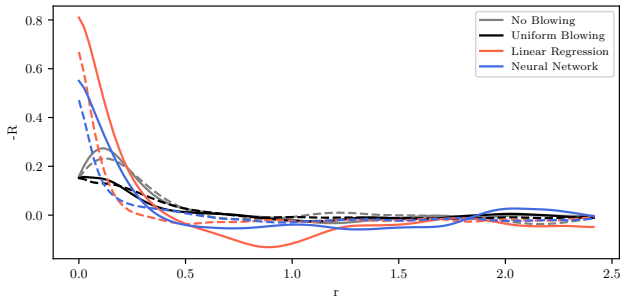

Figure 7. Normalized cross-correlation between wall-normal velocity and pressure fluctuations at the wall split into two different regions. The solid line corresponds to $30 < x < 39.75$ and the dashed line to $39.75 < x < 49.5$.

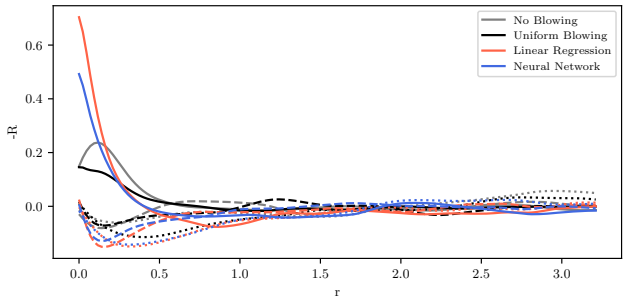

Figure 8. Normalized cross-correlation between wall-normal velocity and pressure fluctuations at varying distances from the wall. The solid line corresponds to $y = 0.003$, the dashed line to $y = 0.43$, and the dotted line to $y = 1.59$.

CONCLUSIONS AND FUTURE WORK

Accurate modeling of transpiration cooling systems is made difficult by the necessary coupling of the turbulent boundary layer and the flow in the porous wall, which differ significantly in time length scales. Herein a method of indirect coupling was proposed where in the flow in the porous medium is reduced to either a representative linear expression or a trained convolutional neural network.

The linear expression obtained using regression was found to significantly attenuate all of the naturally occurring pressure fluctuations, however this is theorized to be a non-physical result due to the significant error of the linear regression where the pressure overly deviates from the mean resulting in an artificial decorrelation of the pressure signal.

The results of the neural network case were much more promising, suggesting the importance of including the spatial influence of neighbouring pores when trying to capture the flow through the porous medium. While the high frequency pressure fluctuations were attenuated in the first quarter of the transpiration region due to this spatial influence, the lower frequency fluctuations persisted throughout the domain.

The influence of neighbouring pores served to dampen the impact of the coupling between the coolant injection velocity and the wall pressure fluctuations when compared with the linear regression case, resulting in a blowing ratio distribution closer to that of the uniform case as well as a reduced cross-correlation between the two signals.

Future work will focus on understanding the observed attenuation of the wall pressure signal via a spectral analysis. The impact on the formation of coherent turbulent structures

as well as on coolant film accumulation and cooling effectiveness will also be explored.

One significant area that warrants further study is the transient effects of flow in the porous medium. In the present work the response time of the flow in the porous medium was assumed to be negligible due to the incompressible nature of the flow within the pores. This allowed a Darcy flow approximation to be used such that the flow in the pores is independent of its previous state. The validity of this assumption for the case of transpiration cooling should be explored further.

Furthermore, it has been shown that the bulk properties which govern flow in the porous medium (permeability, effective porosity and tortuosity) are strongly influenced by the frequency of the imposed pressure signal (Champoux & Allard, 1991). The importance of this effect on interactions of the flow in the porous medium with the turbulent fluctuations in the boundary layer is an important avenue of further investigation.

REFERENCES

Bermejo-Moreno, Iván, Bodart, Julien, Larsson, Johan, Barney, Blaise M., Nichols, Joseph W. & Jones, Steve 2013 Solving the compressible Navier-Stokes equations on up to 1.97 million cores and 4.1 trillion grid points. In *SC '13: Proceedings of the International Conference on High Performance Computing, Networking, Storage and Analysis*, pp. 1–10. ISSN: 2167-4337.

Cerminara, Adriano 2023 Turbulence Effect on Transpiration Cooling Effectiveness Over a Flat Plate in Hypersonic Flow and Sensitivity to Injection Parameters. *Flow, Turbulence and Combustion* **110** (4), 945–968.

Cerminara, Adriano, Deiterding, Ralf & Sandham, Neil 2020 A mesoscopic modelling approach for direct numerical simulations of transition to turbulence in hypersonic flow with transpiration cooling. *International Journal of Heat and Fluid Flow* **86**, 108732.

Champoux, Yvan & Allard, Jean-F. 1991 Dynamic tortuosity and bulk modulus in air-saturated porous media. *Journal of Applied Physics* **70** (4), 1975–1979.

Christopher, Nicholas, Peter, Johannes M. F., Kloker, Markus J. & Hickey, Jean-Pierre 2020 DNS of turbulent flat-plate flow with transpiration cooling. *International Journal of Heat and Mass Transfer* **157**, 119972.

Dahmen, W., Gotzen, T., Müller, S. & Rom, M. 2014 Numerical simulation of transpiration cooling through porous material. *International Journal for Numerical Methods in Fluids* **76** (6), 331–365, _eprint: https://onlinelibrary.wiley.com/doi/pdf/10.1002/fld.3935.

Eckert, E. R. G. & Livingood, N. B. 1954 Comparison of effectiveness of convection-, transpiration-, and film-cooling methods with air as coolant. *Tech. Rep.* NACA-TR-1182. National Advisory Committee for Aeronautics, nTRS Document ID: 19930092205 NTRS Research Center: Legacy CDMS (CDMS).

Esser, Burkard, Barcena, Jorge, Kuhn, Markus, Okan, Altug, Haynes, Lauren, Gianella, Sandro, Ortona, Alberto, Liedtke, Volker, Francesconi, Daniele & Tanno, Hideyuki 2016 Innovative Thermal Management Concepts and Material Solutions for Future Space Vehicles. *Journal of Spacecraft and Rockets* **53** (6), 1051–1060, publisher: American Institute of Aeronautics and Astronautics.

Gostick, Jeff, Aghighi, Mahmoudreza, Hinebaugh, James, Tranter, Thomas, Hoeh, Michael, Day, Harold, Sharqawy, Mostafa, Spellacy, Brennan, Bazylak, Aimy, Burns, Alan, Lehnert, Werner & Putz, Andreas 2016 OpenPNM: A Pore Network Modeling Package. *Computing in Science & Engineering* **18**, 1–1.

Grasso, G., Jaiswal, P., Wu, H., Moreau, S. & Roger, M. 2019 Analytical models of the wall-pressure spectrum under a turbulent boundary layer with adverse pressure gradient. *Journal of Fluid Mechanics* **877**, 1007–1062.

Grasso, Gabriele, Wu, Hao, Orestano, Susanna, Sanjosé, Marlène, Moreau, Stéphane & Roger, Michel 2021 CFD-based prediction of wall-pressure spectra under a turbulent boundary layer with adverse pressure gradient. *CEAS Aeronautical Journal* **12** (1), 125–133, publisher: Springer.

Gülhan, A. & Braun, S. 2011 An experimental study on the efficiency of transpiration cooling in laminar and turbulent hypersonic flows. *Experiments in Fluids* **50** (3), 509–525.

Hillcoat, Sophie & Hickey, Jean-Pierre 2021 Pressure fluctuations under a turbulent boundary layer with transpiration cooling. American Institute of Aeronautics and Astronautics.

Jiao, Longyin & Floryan, J. M. 2021 On the use of transpiration patterns for reduction of pressure losses. *Journal of Fluid Mechanics* **915**, A78.

Jiménez, Javier, Hoyas, Sergio, Simens, Mark P. & Mizuno, Yoshinori 2010 Turbulent boundary layers and channels at moderate Reynolds numbers. *Journal of Fluid Mechanics* **657**, 335–360.

Jin, Ping, Chen, Zhiwei, Sun, Jiguo & Cai, Guobiao 2023 Investigation of full-scale porous injector plate transpiration cooling coupled with combustion in high-thrust H2/O2 rocket engines. *Applied Thermal Engineering* **230**, 120669.

König, Valentina, Rom, Michael & Müller, Siegfried 2021 A Coupled Two-Domain Approach for Transpiration Cooling. In *Future Space-Transport-System Components under High Thermal and Mechanical Loads: Results from the DFG Collaborative Research Center TRR40* (ed. Nikolaus A. Adams, Wolfgang Schröder, Rolf Radespiel, Oskar J. Haidn, Thomas Sattelmayer, Christian Stemmer & Bernhard Weigand), pp. 33–49. Cham: Springer International Publishing.

Liu, Xue, Zhou, Weixing & Yu, Wenli 2023 Numerical simulation study of transpiration cooling with hydrocarbon fuel as coolant. *Applied Thermal Engineering* **221**, 119687.

Prokein, Daniel 2021 Numerical and experimental investigations on transpiration cooling. doctoralThesis, accepted: 2022-09-05T10:15:09Z ISBN: 9781815799440.

Wang, Wenkang, Lozano-Durán, Adrián, Helmig, Rainer & Chu, Xu 2022 Spatial and spectral characteristics of information flux between turbulent boundary layers and porous media. *Journal of Fluid Mechanics* **949**, A16.

Zhang, Zhihui (), Wu, Xiaoyu () & Wang, Xian () 2022 Near-wall vortices and thermal simulation of coupled-domain transpiration cooling by a recursive regularized lattice Boltzmann method. *Physics of Fluids* **34** (10), 107105.

Zhu, Yinhai, Peng, Wei, Xu, Ruina & Jiang, Peixue 2018 Review on active thermal protection and its heat transfer for airbreathing hypersonic vehicles. *Chinese Journal of Aeronautics* **31** (10), 1929–1953.